NUMERICAL ANALYSIS OF THE LOAD-DEFLECTION CHARACTERISTIC OF PNEUMATIC BEAM STRUCTURES

C.G. RICHES* & P.D. GOSLING
Department of Civil Engineering
University of Newcastle-upon-Tyne,
Cassie Building,
Newcastle NE1 7RU
UK
Telephone: + 44 (0) 191 222 5456
Fax: + 44 (0) 191 222 6502
c.g.riches@newcastle.ac.uk
p.d.gosling@newcastle.ac.uk

ABSTRACT

Air inflated beam structures may be used as an alternative to structures fabricated from conventional materials in cases where limiting constraints are placed on rate of assembly and, more significantly, structural mass. Unlike conventional structures, linear elastic theories do not apply. To the contrary, inflatable structures demonstrate strong geometric non-linearity arising from large displacements and potential fabric wrinkling. In addition, the fabric material usually exhibits strong orthotropy.

In order to investigate the possibilities of inflatable structural forms and to fulfil their design potential, a reliable analysis tool is required. This paper presents a mixed or hybrid approach to the numerical analysis of pneumatic beam structures. A geometrically non-linear triangular finite element formulation, used to discretise the pressurised membrane, is described. This element formulation, coupled with the Dynamic Relaxation algorithm, is used to provide solutions to the deflections and stresses for a number of air-inflated cantilever, arch and beam structures both before and after wrinkling of the orthotropic fabric material. The numerical method is shown to lead to a smooth and computationally efficient solution procedure, in which the static problem is effectively replaced by a pseudo dynamic equivalent.

1.0 Introduction

Pneumatic structures, where pressure differentials wholly or largely ensure stability, have the potential to be considered as structurally efficient alternatives to conventional forms in situations where volume and mass are important or where rate of assembly is a factor. This may include structures required to cover or span large areas, structures to be used as emergency shelters, fluid retaining structures, deployable structures for the military, slides for rapid aircraft evacuation and many others. The recent and potential uses of air structures have been well documented (Otto, 1962; Leonard, 1974; Herzog, 1976; Dent, 1971;). In his book Tensile Structures Frei Otto describes a myriad of uses for both air-supported and air-inflated structural forms.

One of the more interesting applications of the pneumatic structure discussed is the use of inflated cylindrical tubes as structural members. These air-inflated structural members lend themselves to situations where ease and rate of construction, as well as structural mass are crucial. Proposals have been made to use complex skeletal inflatables as large deployable space structures to support antenna reflectors (Girard *et al*., 1982; Reibaldi, 1985; Authier and Hill, 1985) and solar concentrators (Grosman and Williams 1989).

Structural Analysis of these inflated cylindrical beams have been performed using a number of different strategies. Research into the structural performance of inflated cantilevered beams under bending, torsion and buckling (Topping 1964; Bulson 1973; Webber 1982) have been undertaken. Non-linear methods have also been used to model the stiffness of inflated cantilevered beams (Douglas 1969). Linear shell analyses have been used to model the buckling behaviour of inflated members (Leonard *et al*. 1960) in which an expression for the collapse load of a cantilevered beam is derived. Comer and Levy (1963) modelled the behaviour of cylindrical cantilever beams between incipient buckling and final collapse, in a manner similar to conventional beam theory. They derived an expression for the deflection of a cylindrical cantilever beam in terms of two dimensionless variables, which when solved gave the beam deflections. Main *et al.* (1992) reformulated this method using a model more applicable to fabric structures. These two papers used a classical solution to find the deflections and stresses under bending based upon conventional beam theory with an assumed stress distribution in the beam. Main *et al*. continued this work with two further papers (Main *et al*. 1994; Main *et al*. 1995) in which a revised bending model is formulated to take into account the biaxial state of stress within the structure.

Numerical solutions to the specific problem of establishing the load-deflection characteristics of pneumatic beams have not, however, been investigated in any great depth. Of the limited papers published Kawabata and Ishii (1994) used a non-linear finite element formulation to analyse a number of air-inflated beam structures.

In this paper, an iterative technique is used to find the load deflection characteristics of inflated, cylindrical beams. Triangular elements are used with a Dynamic Relaxation algorithm to solve for the displacements and stresses during both the pressurisation and loading phases of each pneumatic beam.

2.0 The Numerical Formulation

2.1 Element Formulation

A plane, three noded constant strain triangle has been adopted as the basis of the numerical formulation. In its standard form the constant strain triangle is

defined with six degrees of freedom - *u* and *v* displacements at each node. By assuming three orthogonal degrees of freedom at each node and reselecting the degrees of freedom as extensions of the three sides of the element, the complexity of the element stiffness matrix is reduced. More significantly in the case of the current class of problem, the choice of degrees of freedom enables the continuous membrane to be represented by an equivalent cable net, the analysis of which is computationally efficient in comparison to a conventional plane stress problem. Geometric nonlinearity may also be easily introduced.

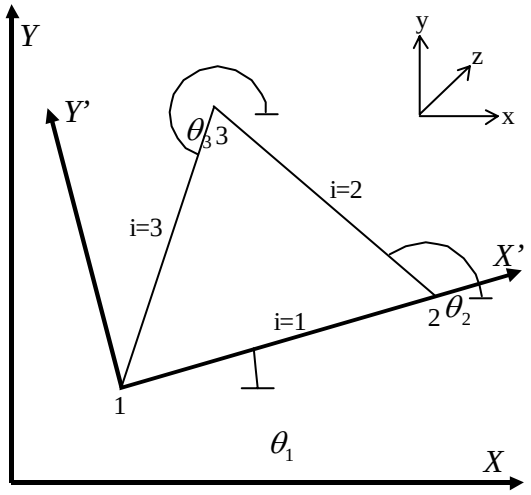

Figure 1: The Triangular Element in the local and global co-ordinate systems.

A full description of the numerical formulation is given in previous work (Gosling and Riches, 1997).

The triangular element is formulated in a local 2 dimensional plane. The local X' and Y' axes of the element lie in the same plane as the *X* and *Y* axes in which the material properties and stress state are defined (Figure 1). The strains in the *X* and *Y* directions are defined as ε_X and ε_Y respectively with the shear strain as γ_{XY}. The side extensions of the triangular element are $\delta_{1,2,3}$ for the three sides.

The local Z' direction is defined to be normal to the surface of the element and calculated as:

$$\vec{Z} = 1\vec{2} \times 1\vec{3} = \begin{vmatrix} i & j & k \\ (x_2 - x_1) & (y_2 - y_1) & (z_2 - z_1) \\ (x_3 - x_1) & (y_3 - y_1) & (z_3 - z_1) \end{vmatrix} \quad (1)$$

where $\{\{x_1, y_1, z_1\}, \{x_2, y_2, z_2\}, \{x_3, y_3, z_3\}\}$ are the global co-ordinates of the element side intercepts $\{\{i_3, i_1\}, \{i_1, i_2\}, \{i_2, i_3\}\}$ respectively. The vector defining the local Y' direction is calculated by the cross product of the vectors $\vec{X}_{tr}$ and $\vec{Z}_{tr}$, where $\vec{X}_{tr}$ is a vector in the local X direction. Using these three vectors the transformation matrix relating the local co-ordinate system to the global system is found:

$$\hat{X}_{tr} = \frac{\vec{X}_{tr}}{|\vec{X}_{tr}|} = \{l_1, m_1, n_1\} \quad (2)$$

$$\hat{Y}_{tr} = \frac{\vec{Y}_{tr}}{|\vec{Y}_{tr}|} = \{l_2, m_2, n_2\} \quad (3)$$

$$\hat{Z}_{tr} = \frac{\vec{Z}_{tr}}{|\vec{Z}_{tr}|} = \{l_3, m_3, n_3\} \quad (4)$$

which gives:

$$\begin{Bmatrix} X'_i \\ Y'_i \end{Bmatrix} = \begin{bmatrix} l_1 & m_1 & n_1 \\ l_2 & m_2 & n_2 \end{bmatrix} \begin{Bmatrix} X_i \\ Y_i \\ Z_i \end{Bmatrix} \quad (5)$$

The direct strain in each element side, *i* is used to solve for the local strains, $\bar{\varepsilon}$:

$$\bar{\varepsilon} = \begin{Bmatrix} \varepsilon_X \\ \varepsilon_Y \\ \gamma_{XY} \end{Bmatrix} =$$

$$\frac{1}{|\bar{A}|}\begin{bmatrix}(b_2c_3-b_3c_2)/l_1 & (b_3c_1-b_1c_3)/l_2 & (b_1c_2-b_2c_1)/l_3\\ (a_3c_2-a_2c_3)/l_1 & (a_1c_3-a_3c_1)/l_2 & (a_2c_1-a_1c_2)/l_3\\ (a_2b_3-a_3b_2)/l_1 & (a_3b_1-a_1b_3)/l_2 & (a_1b_2-a_1b_2)/l_3\end{bmatrix}\begin{Bmatrix}\delta_1\\ \delta_2\\ \delta_3\end{Bmatrix} \quad (6)$$

or

$$\bar{\varepsilon} = \bar{B}.\bar{\delta} \quad (7)$$

where $a_i = \cos^2\theta_i$, $b_i = \sin^2\theta_i$ and $c_i = \sin\theta_i.\cos\theta_i$ and $\bar{B}$ is the matrix relating the element extensions to the element strains.

The elasticity matrix relating the element strains to the element stresses is denoted as $\bar{E}$. If an orthotropic material is to be considered then the coefficients of $\bar{E}$ are:

$$d_{11} = \frac{E_X}{(1-v_{XY}.v_{YX})};\ d_{22} = \frac{E_Y}{(1-v_{XY}.v_{YX})}$$
$$d_{12} = v_{YX}.d_{11};\ d_{21} = v_{XY}.d_{22};\ d_{33} = G_{XY} \quad (8)$$

where E_X and E_Y are the Young's modulus in the X and Y directions, v_{XY} and v_{YX} are the poisons ratio in both directions and G_{XY} is the Shear modulus of the material.

The element elastic stiffness matrix, $\bar{K}_E$, can be found directly from Finite Element Theory, noting that $\bar{B}$ is independent of the local co-ordinates and assuming a constant thickness:

$$\underset{(3x3)}{\bar{K}_E} = \bar{B}^T.\bar{E}.\bar{B}.V \quad (9)$$

where V is the volume of the element.

The geometric stiffness matrix, $\bar{K}_\sigma$, models the contribution of the forces within the element to the overall stiffness of the element.

The geometric stiffness is obtained using pseudo cables that are analogous to the geometric stiffness of the linear or bar element.

The longitudinal direction of a bar element in the global co-ordinate system can be specified by the unit vector $\hat{c}$, given by the components:

$$\hat{c} = \begin{bmatrix}c_x\\ c_y\\ c_z\end{bmatrix} = \frac{1}{l}\begin{bmatrix}x_2-x_1\\ y_2-y_1\\ z_2-z_1\end{bmatrix} \quad (10)$$

where c_x, c_y and c_z are the direction cosines in the x, y and z directions.

Using these relationships and the moment generated by the element force, P_N, it can be shown that the element geometric stiffness matrix is equal to:

$$\bar{K}_\sigma = \frac{P_N}{l}\begin{bmatrix}\bar{I}_3-\hat{c}.\hat{c}^t & -(\bar{I}_3-\hat{c}.\hat{c}^t)\\ -(\bar{I}_3-\hat{c}.\hat{c}^t) & \bar{I}_3-\hat{c}.\hat{c}^t\end{bmatrix} \quad (11)$$

The element side force, P_N, is comprised of components due to the elastic straining and due to any initial prestress, $\bar{\sigma_o}$. The natural force, P_N, may be related to the element stresses from which the natural element force, P_N, can be expressed as:

$$\bar{T_o} = \begin{Bmatrix}T_1\\ T_2\\ T_3\end{Bmatrix} = V.\bar{B}^T.\bar{\sigma_o} \quad (12)$$

where $\bar{T_o}$ is the vector of element side forces representing the initial stress, $\bar{\sigma_o}$, within the element.

The total stiffness matrix of the triangular element is obtained by combining the elastic and geometric stiffness matrices as in:

$$\bar{K} = \bar{K}_E + \bar{K}_\sigma \quad (13)$$

The continuum based triangular element can be represented by a triplet of pseudo cables possessing the elastic and geometric properties described above. The continuum is effectively replaced with a cable net (or bar net due to the admissibility of compressive natural

forces) whose stress field represents that of a continuum through the natural forces and stiffness in the cables.

2.2 The Dynamic Relaxation Algorithm

The Dynamic Relaxation algorithm is a method of solution based upon the principle that any body that is in motion will come to rest when it is in a state of equilibrium. A system of simultaneous equations is set up using this principle and the equations of dynamic equilibrium of a body in motion. These equations of dynamic equilibrium are given by:-

$$P_{pq} = M_{pq}.\ddot{\delta}_{pq} + C.\dot{\delta}_{pq} + \underline{K}_{pq}.\delta_{pq} \quad (14)$$

or alternatively:

$$\underline{P}_{pq} - \underline{K}_{pq}.\delta_{pq} = M_{pq}.\ddot{\delta}_{pq} + C.\dot{\delta}_{pq} \quad (15)$$

and:

$$\underline{R}_{pq} = M_{pq}.\ddot{\delta}_{pq} + C.\dot{\delta}_{pq} \quad (16)$$

where $\underline{P}_{pq}$ = the external load vector
$\underline{K}_{pq}$ = the nodal stiffness
$\underline{R}_{pq}$ = the out of balance nodal force
M_{pq} = the fictitious nodal mass
$\ddot{\delta}, \dot{\delta}$ and δ = the nodal acceleration, velocity and displacement
C= the viscous damping coefficient

The subscripts p and q refer to the p^{th} node in the q^{th} direction. The subscript q can take values 1-3 corresponding to the x, y and z directions respectively.
Equation (16) describes a pseudo-dynamic behaviour in which the structure oscillates about a position of equilibrium with gradually reducing amplitude, due to viscous damping. A more stable and efficient technique is kinetic damping, where the movements of the structure are arrested whenever a kinetic energy peak is detected. This results in a simplification of Equation (16) in which C is taken as zero:

$$M_{pq}.\ddot{\delta}_{pq} = \underline{R}_{pq} = \underline{P}_{pq} - \underline{K}_{pq}.\delta_{pg} \quad (17)$$

After each energy peak is detected the current geometry is set and the whole process is re-started.
The acceleration term in Equation (17) is the variation of velocity over a time increment δt using a central difference approximation. This leads to a recurrent equation for the nodal velocity:

$$\dot{\delta}_{pq}^{t+\frac{\delta t}{2}} = \dot{\delta}_{pq}^{t-\frac{\delta t}{2}} + \underline{R}_{pq}^{t}.\frac{\delta t}{M_{pq}} \quad (18)$$

To ensure numerical stability of the algorithm it has been suggested (Barnes 1982) that the time increment δt should be such that:

$$M_{pq} \le \frac{1}{2}.\underline{K}_{pq}.\delta t^2 \quad (19)$$

Substitution of Equation (19) into Equation (18) gives:

$$\dot{\delta}_{pq}^{t+\frac{\delta t}{2}} = \dot{\delta}_{pq}^{t-\frac{\delta t}{2}} + \underline{R}_{pq}^{t}.\left(\frac{2}{\delta t.\underline{K}_{pq}}\right) \quad (20)$$

Using these velocities at time $t+\frac{\delta t}{2}$ the current nodal displacements can also be found using:

$$\delta_{pq}^{t+\frac{\delta t}{2}} = \dot{\delta}_{pq}^{t+\frac{\delta t}{2}}.\delta t \quad (21)$$

The pseudo-dynamic behaviour of the structure can be described using the Equations (17), (20) and (21).

The current kinetic energy, $U_k^{t+\frac{\delta t}{2}}$, is calculated using:

$$U_k^{t+\frac{\delta t}{2}} = \frac{1}{2}\sum_{p=1}^{p=N}\sum_{q=1}^{q=3} M_{pq}(\dot{\delta}_{pq}{}^{t+\frac{\delta t}{2}})^2 \quad (22)$$

where *N* is the total number of nodes in the discretised system.

An energy peak is deemed to have occurred in the time interval if the magnitude of the current kinetic energy is less than that of the preceding value.

With the Dynamic Relaxation Algorithm the out of balance forces at each node are divided by the direct component of element stiffness, from all elements meeting at that node, in order to calculate the nodal velocity. The required stiffness term should be determined from the sum of the element stiffness matrices meeting at the relevant node. This matrix should then be inverted to yield the direct flexibility terms taking into account the coupling effects of the all the degrees of freedom. However as the determinant of an unconstrained element is zero, this cannot be achieved. It is therefore only the diagonal terms of element stiffness matrices that are summed at each node.

2.3 The Inflated Cantilever Beam Model

The non-linear behaviour of an inflated beam structure is represented within the numerical model.

The model takes into account the nature of material used in pneumatic structures and the possibility of fabric wrinkling whereby compressive stresses are inadmissible (this should not be confused with admissible compressive forces in the bar elements). The principle stresses in each element are calculated and monitored. If one or both of the principle stresses are found to be negative, the element stresses (σ_x, σ_y and τ_{xy}) are recalculated, with any negative principle stresses set to a value close to zero. The element side forces and the geometric stiffness are then recalculated using this modified stress field.

The internal pressure present is represented within the model. The analysis is performed with an equivalent loading pattern representing the internal pressure present within the structure.

This loading pattern is calculated using the local co-ordinate system of each of the elements within the structure. The internal pressure acts normal to the surface, or in the local Z' direction, of each element. Using the transformation matrix, defined in the initial element formulation, these normal loads can be transformed into the global system, in order that loads arising from a number of arbitrarily orientated elements can be combined.

Nodal loads due to internal pressure can be applied to any structure that can be described using the triangular elements. Any changes in nodal loads that occur because of changes in the surface geometry of the structure, due to external loads or the pressure itself, can also be modelled.

In order to model the effects of the internal pressure upon the cylindrical beam accurately the numerical method has two distinct stages; 1. pressurisation and 2. loading. Once equilibrium is attained in the pressurisation phase any external point loads are applied and the algorithm is restarted.

3.0 Numerical Results

In order to verify the numerical model presented, initial analyses of an inflated cylindrical cantilever model were carried out and compared with numerical results obtained using the commercially available LUSAS Finite Element package (Figure 2).

A quadratic, triangular semi-loof shell element and a Total Lagrangian incremental and iterative solution method

were used in the LUSAS analysis. As the LUSAS package does not include a no-compression model, the results were obtained at loads below the expected wrinkling load of an inflated cylindrical cantilever beam.

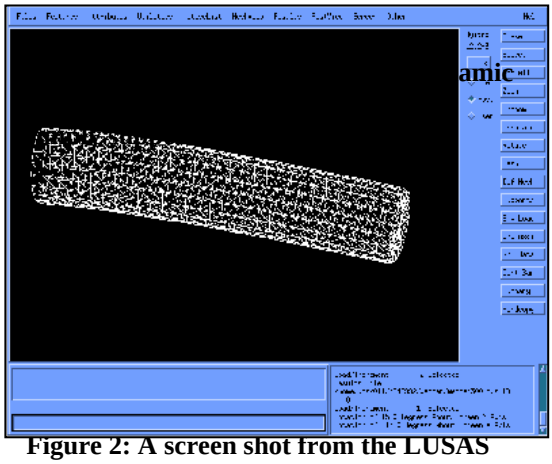

Figure 2: A screen shot from the LUSAS Finite Element package.

A numerical analysis, using Dynamic Relaxation, of the 300mm diameter inflated cantilever, subject to an internal pressure of 16,900 N/mm^2 was carried out and compared with the results obtained using the commercial package.

Table 1: Deflections of 300mm diameter cylindrical cantilever.

Load (N)	Deflection (mm)	Nonlinear Deflection from LUSAS (mm)
5	1.438	1.436
10	2.876	2.872
15	4.313	4.308
20	5.749	5.744
25	7.184	7.719
30	8.618	8.608
35	10.05	10.04
40	11.48	11.48
45	12.91	12.91
50	14.34	14.35

It can be seen that there is extraordinarily good correlation between the results obtained using the LUSAS Finite Element package and those obtained using the numerical technique presented.
These initial results show that the triangular element presented is appropriate for the analysis of this class of problem.
Further analyses were carried out, using Dynamic Relaxation, on inflated cylindrical cantilever and simply supported beam models of length 400mm and radius 25mm. In the analyses the material was assumed to be isotropic and the Young's modulus and Poisson's ratio were set as 4x10^3 N/mm^2 and 0.1 respectively.
The axial tension in a cylindrical beam, in the range of linear theory, subject to bending can be expressed as:

$$N_x = \frac{pr}{2t} \pm \frac{Mr}{I} \qquad (23)$$

where: p = internal pressure
r = radius of cylinder
t = material thickness
M = bending moment
I = the second moment of area
$= \pi r^3 t$ for a circular tube

The first part of Equation (23) represents the longitudinal pre-stress caused by inflation, the second part the stresses induced by bending.
Incipient wrinkling of a fabric cylindrical beam will occur when N_x becomes negative.
The wrinkling of an inflated cantilever beam, subject to a laterally applied end load will begin when the load, P_w, exceeds:

$$P_w = \frac{\pi p r^3}{2l} \qquad (24)$$

The wrinkling load in a simply supported beam subject to a centrally applied point load is given by:

$$P_w = \frac{2\pi p r^3}{l} \qquad (25)$$

For the cylindrical cantilever beam analysed subject to an internal pressure of 0.035 N/mm^2, incipient wrinkling should

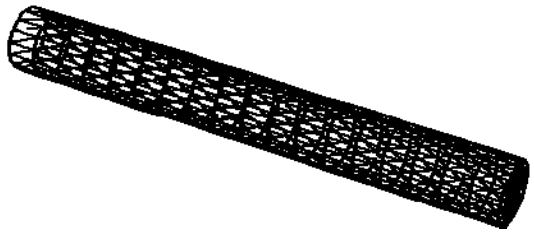

occur at a load of 2.15 N. The wrinkling load of the simply supported beam analysed will therefore be 8.6 N.

Theoretical collapse of the beams will occur when the longitudinal stress around the circumference of the cylinder is equal to zero.

It can be seen that for a constant externally applied moment, *M*, wrinkling of cylindrical inflatable will occur when the internal pressure, *p*, drops below:

$$p = \frac{2M}{\pi r^3 t} \qquad (26)$$

Incipient wrinkling of the cantilever and simply supported beams, analysed with a constant applied moment, will occur as the internal pressure drops below 0.1 and 0.15 N/mm^2 respectively.

Two separate numerical analyses were carried out on each of the cylindrical cantilever and simply supported beam structures. Identical meshes were used for both analyses (Figure 3).

The structures were initially analysed subject to a constant internal pressure of 0.035 N/mm^2 and an increasing external load to collapse. In addition an analysis of the structures subject to a varying internal pressure and constant point load was also carried out. The cantilever and simply supported beams were subject to a constant point loads of 5.0 N and 50.0 N respectively.

The load-deflection characteristics of these two beam structures can be seen in Figure 4 and Figure 5.

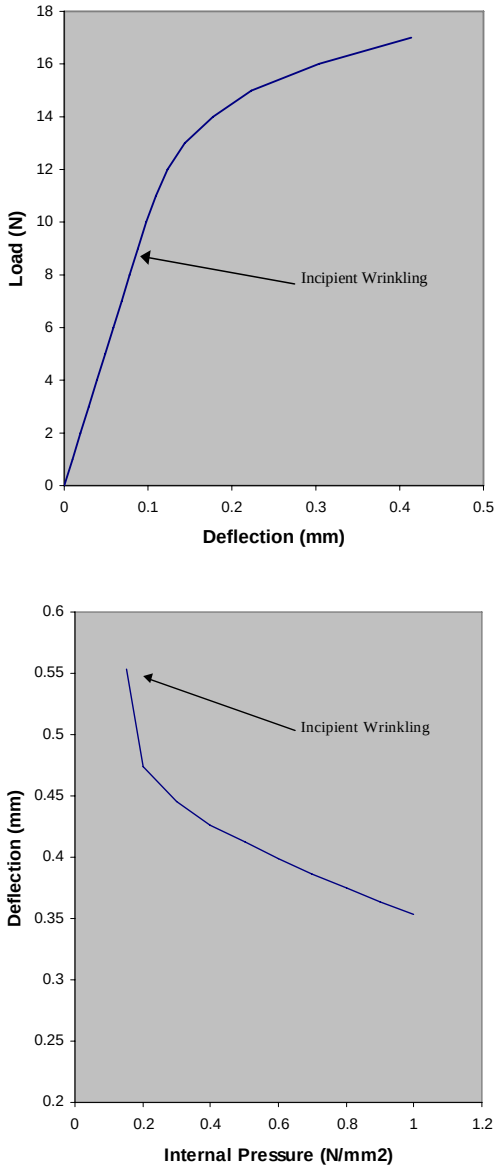

Figure 4: The Load-Deflection and Internal Pressure-Deflection characteristics of an inflated simply supported beam.

The deformation of a semi-circular arch has also been investigated (Figure 6). A 12m span, 400mm radius arch structure was analysed using the numerical method inflated to a constant internal pressure of 0.01N/mm^2 with a centrally applied external load. From the numerical analysis incipient wrinkling of the arch structure occurs at an approximate load of 600 N (Figure 7).

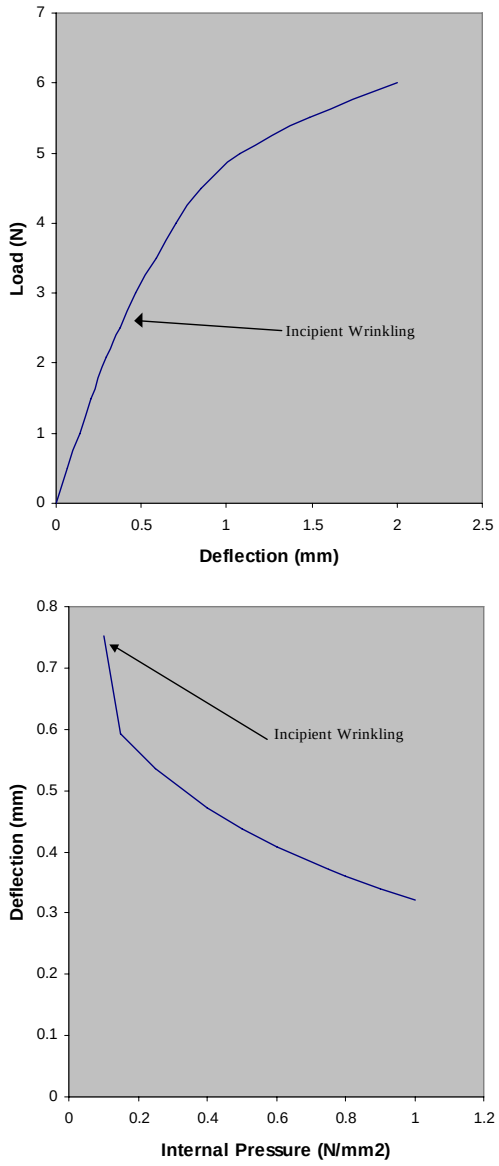

Figure 5: The Load-Deflection and Internal Pressure-Deflection characteristic of an inflated cylindrical cantilever beam.

4.0 Conclusions

A Geometrically non-linear numerical method has been used to provide solutions to the load-deflection characteristics of a number of inflated cylindrical beam structures.

The analyses carried out on inflated cantilever and simply supported beams clearly illustrate the effect of fabric wrinkling. The results suggest that, for this class of structure, much of the nonlinearity of the load-deflection curve arise because of, or after, fabric material wrinkling.

The deflections of the cantilever beam structure increase immediately after incipient wrinkling. The deflections of the simply supported beam do not, however, increase to the same extent immediately after wrinkling. This would suggest that the overall stiffness of the simply supported beam is not affected by fabric wrinkling to the same extent as that of the cantilever.

The results indicate a significant decrease in beam stiffness after incipient wrinkling, or local buckling, of the material. The analysis does, however, show that inflated beam structures exhibit considerable load bearing capacity after the onset of wrinkling, arising from a redistribution of bending stresses within the fabric.

The deformation of a semi-circular arch subject to a centrally applied external load has also been investigated. The results of this analysis show a similar load-deflection curve to that of the other inflated beam structures. The arch structure is, however, a more stable form than both the simply supported and cantilever beams. This is illustrated by the fact that fabric wrinkling of the material does not have as great an effect on the deflections and the eventual collapse load in comparison to the previous forms.

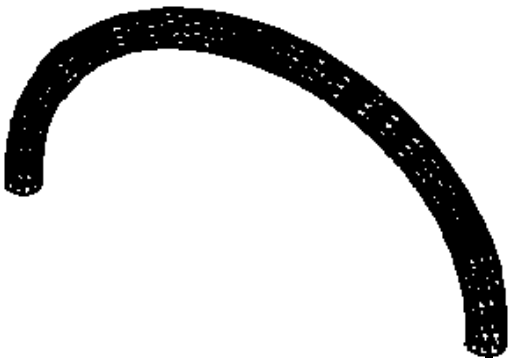

Figure 6: Mesh used in Dynamic Relaxation analysis of inflated arch structure.

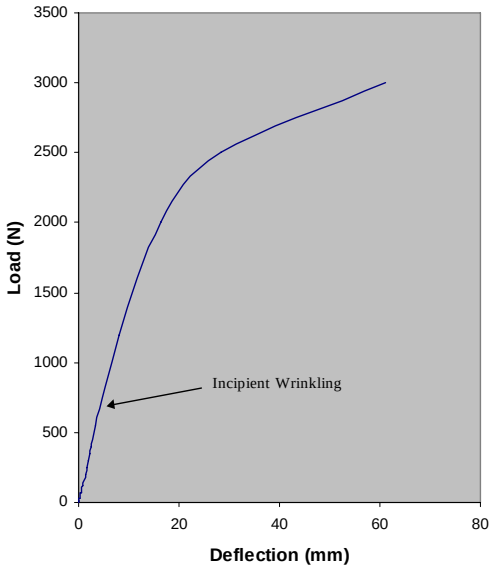

Figure 7: The Load-Deflection characteristic of an inflated arch structure.

The analyses also show the effect of internal pressure and radius of cross section upon structural performance. The internal pressure increases both the cross sectional area, and the shear stiffness of the structure. An increase in radius has the effect of increasing the second moment or area of the beam and also the longitudinal and radial pre-stresses within the fabric due to inflation.

Difficulties arise using this numerical formulation with the dynamic relaxation algorithm, regarding the stability of the algorithm. A considerable amount of time is needed to analyse more complex structures or when geometry or loading patterns change considerably.

Further work is to be carried out using this numerical method to analyse the structural performance of other arch, beam and tent-like air-inflated structures. Further investigation of the structural performance of semi-pneumatic membrane structures, comprising of inflated cellular, tube and pre-stressed membrane elements, is planned.

4.0 References

Authier, B. and Hill, L. (1985), "Large Inflatable parabolic reflectors in space", Instrumentation for Submillimeter Spectroscopy, pp. 126-132

Barnes, M. (1982), "Non-linear numerical solution methods for static and dynamic relaxation", IL Publication Number 15, pp. 150-166.

Bulson, P.S. (1973), "Design principles of pneumatic structures", The Structural Engineer, Vol. 56, No. 6, pp. 209-215

Comer, R.L. and Levy, S. (1963), "Deflections of an inflated circular-cylindrical beam" AIAA Journal, Vol. 1, No. 7, pp. 1652-1655.

Douglas, W.J. (1969),"Bending Stiffness of an inflated cylindrical cantilever beam", AIAA Journal, Vol. 7, No.7, pp. 1248-1253.

Girard , L., Bloetscher, F. and Stimler, F. (1982), "Innovative structures for space applications", Goodyear Aerospace Rep. GAC 19-1563; NTIS N84-25757, Washington, DC

Gosling, P.D. and Riches, C.G. (1997), "Some results on the Load-Deflection Characteristics of Pneumatic Beams", Proceedings IASS International Symposium on Shell and Spatial Structures, Singapore

Grossman, G. and Williams, G. (1989), "Inflatable concentrators for solar propulsion and dynamic space power", Solar Engrg.-1989; Proceedings of the 11th Annual ASME Solar Energy Conference, American Society of Mechanical Engineers, New York, NY.

Kawabata, M. and Ishii, K. (1994), "Study on Structural Characteristics of Air-Inflated Beam Structures", Proc of IASS-ASCE Int Symp on Spatial, Lattice and Tension Struct, Atlanta, pp. 742-751

Leonard, J.W. (1974), "State of the art in inflatable shell research", Journal of the Engineering Mechanics Division, ASCE, Vol. 100, No.1, pp. 17-25.

Leonard, R.W., Brooks, G.W. and McComb, H.G. (1960), "Structural Considerations of Inflatable Reentry Vehicles", NASA TN D-457

Main , J.A., Peterson, S.W. and Strauss, A.M. (1992), "Beam-type bending of space-based inflated membrane structures", Journal of Aerospace Engineering, Vol.8, No.2, pp. 120-128

Main , J.A., Peterson, S.W. and Strauss, A.M. (1992), "Load-deflection behaviour of space-based inflatable fabric beams" Journal of Aerospace Engineering, Apr 1994, Vol.7, No.2, pp. 225-238

Main , J.A., Peterson, S.W. and Strauss, A.M. (1992), "Preliminary structural analysis of space-based inflatable tubular frame structures." American Society of Mechanical Engineers, Petroleum Division , Vol.47, No.1., pp. 115-121

Otto, F. (1962), Tensile Structures, MIT Press, Cambridge, MA.

Reibaldi, G.G. (1985), "Inflatable technology in orbit demonstration within the European space agency programs", Proceedings of the 25th International Conference on Space, Rome, Italy, pp. 199-205.

Topping, A.D. (1964), "Shear Deflections and buckling characteristics of inflated members", Journal of Aircraft, Vol. 1, No. 5, pp. 289-293

Webber, J.P.H. (1982), "Deflections of inflated cylindrical cantilever beams subjected to bending and torsion", Aeronautical Journal, pp. 306-312.